CHAPTER II
THEORETICAL BACKGROUND AND LITERATURE SURVEY

2.1 Artificial Muscles and Actuators

Polymer artificial muscle and actuator technologies are being developed that produce strains and stresses within the materials using electrostatic forces, electrostriction, ion insertion, and molecular conformational changes.

Polymer artificial muscles have been divided into two major groups (Bar-Cohen, 2004). In the first group, the dimensional change (actuation) is the response to an electric field. These are commonly known as electronic or electric electroactive polymers (EAPs). Some of the technologies that fall under this category are dielectric elastomer actuators (DEAs), ferroelectric polymers, and liquid crystal elastomers. The second group of polymer artificial muscles is a class of materials in which the presence and movement of ions is necessary to make actuation possible. This group is referred to as ionic EAPs. For the ions to be able to move, an electrolyte phase is necessary, which is often liquid; so these actuators are also known as wet EAPs (Mirfakarai*et al.*, 2007).

2.2 Electroactive Polymer (EAP)

Electroactive polymer (EAP) is the polymer which can respond to the electric field so EAPs are able to show electrically-induced deformations. These polymers show many outstanding properties, such as sizable active strains and/or stresses in response to an electrical stimulus, low specific gravity, high grade of process ability and down-scalability and, in most cases, low costs. EAP materials can be classified in two major categories (Carpi, 2003):

2.2.1 Ionic EAP (Activated by an Electrically-induced Transport of Ions or Molecules)

- ion polymer metal composites
- conducting polymers
- carbon based reinforcements

2.2.2 Electronic EAP (Activated by an External Electric Field and by Coulombian Forces):

- piezoelectric polymers
- electrostrictive polymers
- dielectric elastomers

Ionic EAPs can be activated advantageously by very low voltages (order of 1 V), but can be operated only within a surrounding electrolyte medium. Differently, electronic EAPs require typically high driving electric field (order of 10-100 V/μm), even though several progresses concerning the reduction of the necessary field are currently occurring. Materials belonging to the two EAP classes present very different properties and actuating performances, leading to the realization of devices showing unlike values of typical figures of merit, such as generable active strains and stresses, required driving voltages, efficiency, lifetime, chemical stability and reliability (Carpi, 2003).

2.3 Conductive Polymers (CPs)

Conductive polymers (Chandrasekhar, 1999) are intrinsically conducting polymers without a presence of any conductive filler. The unique intrinsic conductivity of these organic materials, which generally are comprised simply of C, H and simple heteroatoms such as N and S and the myriad of properties emanating from it arise uniquely from the π-conjugation. Fairly extended and delocalized conjugations originate from the overlap of π-electrons.

This conductivity of CPs (Mirfahrhai *et al.*, 2007) can occur because the electrons are delocalized in the conjugation structure. Most of the CPs have the

structure with alternate between single and double bond. The conductivity of CPs can be achieved through a chemical or electrochemical oxidation or reduction, by a number of anionic or cationic species, called "dopants". Several conductive polymers are shown below:

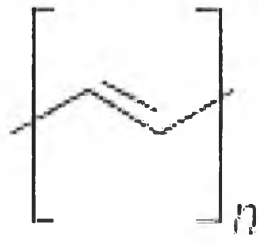

(a) Polyacetylene

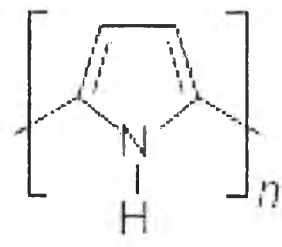

(b) Polypyrrole

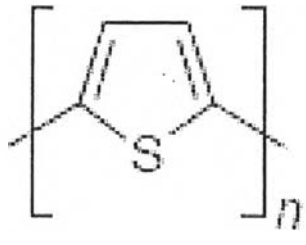

(c) Polythiophene

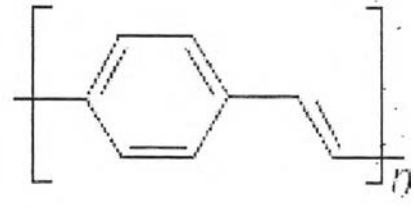

(d) Polyphenylenevinylene

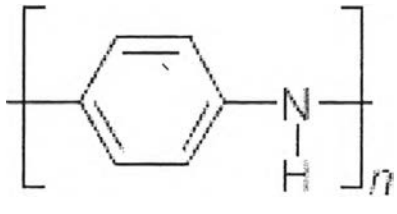

(e) Polyaniline

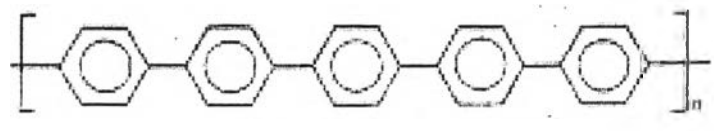

(f) Poly(p-phenylene)

Figure 2.1 Examples of conductive polymers (CPs): (a) Polyacetylene; (b) Polypyrrole; (c) Polythiophene; (d) Polyphenylenevinylene; (e) Polyaniline; (f) Poly(p-phenylene).

Some applications of interest include polymer light-emitting diodes, electrochromic windows, energy storage, sensing and actuation devices (Skotheim *et al.*, 1998).

These conducting polymer artificial muscles use the dimensional changes resulting from electrochemical ion insertion and de–insertion, possibly along with associated solvating species. Since both electrodes can comprise of conducting polymers, both can be used as artificial muscles. Depending upon the conducting polymer/electrolyte system used, the initial state, and the rate of potential change used for actuation, electron insertion into one electrode can be accompanied by a volume increase as cations are inserted or a volume decrease as anions are removed. Similar processes can occur at the counter-electrode. This feature, as well as possible time-dependent changes of the intercalated/deintercalated species, can complicate the control of actuation (Kiefer *et al.*, 2007).

The advantage of conducting polymers over electronic EAPs is their low operating voltage. They feature higher strains and are lower in cost than CNTs. Like CNTs, the electromechanical coupling is low (<1%). Much of the input electrical energy can be recovered, but the need to shunt relatively large amounts of electrical energy can slow actuation and push the limits of power supplies, making large-scale applications (e.g. robotic arms) challenging . One promising means of improving coupling is to design conjugated molecules that fold and expand in response to changes in oxidation state, bringing artificial muscle a little closer to the elegance of real muscle (Mirfakarai *et al.*, 2007).

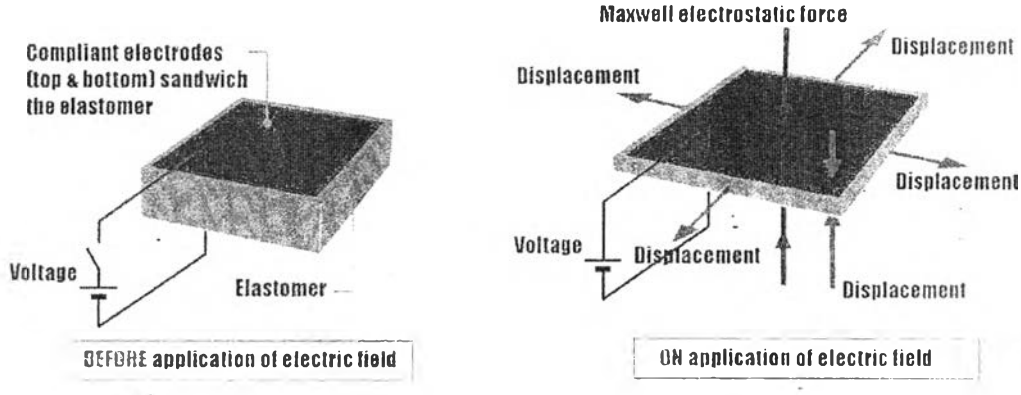

Figure 2.2 Electroactive responses under electric field.

2.4 Conductivity Classification

Materials may be classified into three broad categories according to their room temperature conductivity properties: Insulator, Semiconductors and Conductors.

The overlapping of individual molecular electronics state in all these materials produces electronic bands. Valence electron states overlap to produce a valence band, while the electronic state intermediately above the valence band also coalesces to produce a conduction band. The band gap, generally denoted E_g, is the energy gap between the valence band and the conduction band. If the gap is large, it is more difficult to excite electrons into the conduction band and an insulator results at room temperature.

Normally, thermal excitation at room temperature gives rise to some conductivity in many such inorganic semiconductors. Doped CPs, when in an appropriate oxidized or reduced state, are semiconductors as a result of their unique, extended π-conjugation. Indeed the extended-overlap of π-bands becomes the valence band and the π- bands become the conduction band in CPs. The band gap in most of CPs is about 1 eV (Chandrasekhar, 1999).

Generally, conductive polymers are an insulator (conductivity is less than 10^{-7} S/cm) which have a large band gap. Doping with a weak oxidizing agent or a reducing agent results a diminish of a band gap. According to this reason, less energy

required to stimulate an electron or a hole to jump over from the valence band to the conduction band and an insulator can become a semiconductor which is the conductivity is in the range of 10^{-7} to 10^{2} S/cm (Pratt, 1996).

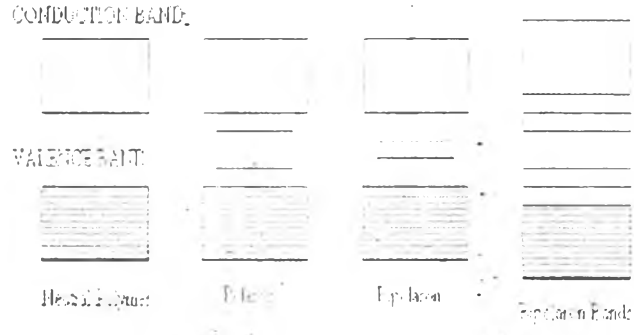

Figure 2.3 Electronic band in neutral, polaron, bipolaron, and bipolaron band in conductive polymers.

2.4.1 Doping

The semiconductor band structure of CPs permits the electronic excitation or the electron removal/addition leading. This process is called doping, and it lead to some interesting properties of CPs.

Oxidation caused by a chemical species generates a positively charged CPs and an associated anion. Oxidation is an anionic doping or the p-type doping. Reduction generates a negatively charged CPs and an associated cation. Reduction is a cationic doping or the n-type doping.

The anionic dopant is an electron rich species: for example chloride, perchlorate and tetrafluoroborate. The cationic dopant is an electron poor specie, such as proton and sodium (Chandrasekhar, 1999).

On the other hand, a new strategy in which dopant was used to stabilize the Ppy as a soluble state was developed. By this strategy, they could prepare Ppy using a simple non-substituted pyrrole and a long alkyl chain-derived dopant such as dodecylbenzene sulfonic acid (DBSA) that is soluble in many organic solvents in a conventional way (Jang *et al.*, 2004; Prissanaroon *et al.*, 2000).

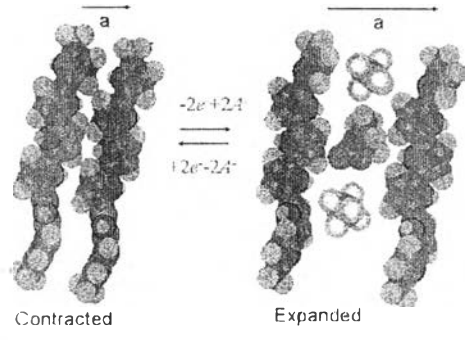

Figure 2.4 Possible mechanism of actuation ion (yellow/purple:A^-) and solvent (red/blue/gray) insertion between chain.

2.5 Polypyrrole (PPy)

Conducting polymers (CPs) have been intensively studied for their one-dimensional conjugated structures and adjustable conductivity. Among the conducting polymers, polypyrrole (PPy) is one of the most investigated due to its high electrical conductivity and its relatively good environmental stability and low toxicity (Prissanaroon *et al.*, 2000).

In 1994, Mansouri found that polypyrrole nanofibers have been synthesized by the electrochemical polymerization with a scanning microneedle electrode or using a microporous membrane as the template.

Comparing with the electrochemical method, the method of in situ doping chemical oxidation polymerization is simpler and cheaper in producing large quantities of nanostructural polypyrrole, because it overcomes the limitation of the area of electrode (He *et al.*, 2003).

Martin (1994) found that the electrical conductivity was enhanced when the diameter of polypyrrole nanotubules decreased, the maximum value of conductivity was over 2000 S/cm.

Duchet *et al.* (1998) used commercial polycarbonate nanoporous particle track-etched membranes as templates to prepare polypyrrole nanotubules and nanofibrils. By nanoporous Polycarbonate (PC) particle track-etch membrane (PTM)

were used as a template membrane for the synthesis of PPy nanostructure. The synthesis of PPy nanostructure has been divided into two synthesis types.

Chemical synthesis: A PC PTM was used a dividing wall in a two-compartment cell. In the first compartment, an aqueous pyrrole solution was added and allowed to diffuse through the membrane to the introduction of the oxidant reagent ($FeCl_3$) in the second compartment. The monomer and the oxidant reagent diffuse toward each other through the pore of the membrane and react to yield the polymer. The membrane was then removed from the cell and rinsed several times with purified water.

Electrochemical synthesis: A metallic layer serving as electrode was evaporated onto one side of the membrane: 10-20 nm adhesion layer of Cr was applied first, followed by a Au film with a thickness of 500 nm to 1μm. Electroplating was performed at room temperature in a conventional one-compartment cell with a Pt counter electrode and a SCE reference electrode at voltage of +0.8 V.

Prissanaroon *et al.* (2000) studied the synthesis and characterization of polypyrrole under the effect of dodecylbenzene sulfonic acid concentration on the electrical properties of polypyrrole thin films in N_2 and SO_2 atmosphere. They found that the conductivity of polypyrrole films was improved by higher doping and SO_2 concentrations and when doping levels was greater than 0.20 M the morphology of polypyrrole changed to fibrillar structure. However, the diameter of fibrils increased with the dopant concentration.

Cuenot *et al.* (2000) found that the elastic modulus strongly increased when the thickness or outer diameter of polypyrrole nanotubules decreased. The nanotubes were mechanically tested in three points bending using atomic force microscopy. The elastic tensile modulus was deducted on different nanotubes with outer diameter ranging between 35 and 160 nm.

Liu and Wan, (2001) attempted a synthesis the nanotubules of PPy doped with naphthalenesulfonic acid. The nanotubules of PPy showed interesting mechanical and conductivity properties.

Ruangchuay *et al.* (2004) investigatd electrical conductivity response of polypyrrole to acetone vapor: effect of dopant anions. Acetone is a flammable

ingredient in a lacquer. This is one of the main causes of fire accident on construction sites and in chemical stores.

Wang *et al.* (2005) studied about Polypyrrole nanoparticles and dye absorption properties. Polypyrrole (PPy) nanoparticles were prepared by using microemulsion polymerization processes at 3 °C. Polypyrrole nanoparticles were dedoped by a 10% NaOH solution, followed by a redoping process using a nuclear fast red kernechtrot dye, which had a sulfonate group. Dedoping changed the optical absorption properties of the nanoparticles. Removal of Cl^- from the surface of PPy nanoparticles was by using NaOH (dedoping). The Cl^- ion acted as a dopant and hence improved the conductivity of the polymer. Partial removal of the dopant anion increased the electrical resistivity of the particles. The red dye solution ($C_{14}H_8NNaO_7S$) was used to redope the nanoparticle. As the red dye has a $-SO_3^-$ group, it was able to function as a dopant anion and improved the conductivity of PPy nanoparticles. PPy nanoparticles were added to a highly concentrated solution of the red dye overnight, resulting in a 20% increase in the electrical conductivity. The dye was used to replace the chloride ion and redoping the particles by dye molecules, which had sulfonic anion groups resulted in improvement of conductivity.

Prissanaroon-Ouajai *et al.* (2008) studied a novel pH sensor based on hydroquinone monosulfonate-doped conducting polypyrrole. PPy films were electropolymerized using hydroquinone monosulfonate (HQS), a compound with a quinhydrone-like structure, as a functional dopant. HQS-doped PPy was electroactive in response to pH changes. HQS-doped PPy showed an excellent potential as a novel pH sensor.

Cuchi *et al.* (2009) studied the preparation and properties of polypyrrole (PPy)-coated silk fabrics: Silk fabrics were coated with electrically conducting doped PPy by the oxidative polymerization from an aqueous solution of pyrrole (Py) at room temperature. The crystalline structure and the molecular conformation of silk were not affected by the polymerization. PPy-coated silk fabrics attained a significantly higher thermal stability than untreated ones, due to the effect of the PPy layer against thermal degradation. PPy-coated silk fabrics displayed excellent electrical properties. The resistance of PPy-coated silk fabrics decreased exponentially with increasing the reaction time or the concentration of PPy in the

reaction system. In this study, new perspectives were open for future applications of PPy-coated silk fabrics, from interactive and smart textiles to innovative bio-based conductive composites for biomedical end-uses.

2.6 Carbon Nanotubes and Graphene

Carbon nano-reinforcements, such as graphite, diamond, fullerenes, carbon nanotubes (CNTs), and graphene, have been applied for various applications in electronic, opticelectronic, sensors, biomedical engineering, medical devices, and actuator. CNTs and graphene belong to the important new carbon family due to their promising properties; electrical, thermal, and mechanical properties. Carbon nanutubes (CNTs) and graphene are two carbon structures which consist of a meshwork of sp^2 carbon atoms, however they have different structure (Du *et al.*, 2014).

CNTs diameters are smaller than conventional carbon or glass fibers about 1000 times. Usually, nanotube aspect ratios are over 1000. The structural characteristics of CNTs are high aspect ratio, high surface area, and excellent mechanical, electrical and thermal properties. The combination of CNTs/polymer composites can be used to enhance their mechanical properties despite undergoing large deformations without damage (Bower *et al.*, 2000).

CNTs provide two morphologies; single-walled carbon nanotube (SWNT) and multi-walled carbon nanotube (MWNT). SWNT and MWNT have been synthesized by various methods; arc discharge and laser ablation methods provide a higher degree of structural perfection but high temperature (> 3000 °C) involved in the synthesis; chemical vapor deposition (CVD) can produce at a lower temperature (< 1000 °C) but with a higher defect in carbon structure, which affects in the electrical and thermal properties (Collins *et al.*, 2000).

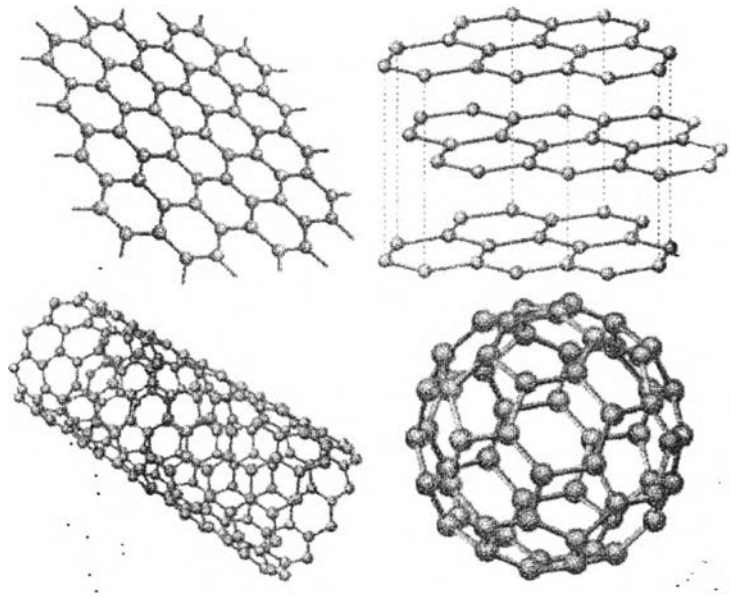

Figure 2.5 Graphene (top left) is a honeycomb lattice of carbon atoms. Graphite (top right) can be viewed as a stack of graphene layers. Carbon nanotubes are rolled-up cylinders of graphene (bottom left). Fullerenes (C60) are molecules consisting of a wrapped graphene through the introduction of pentagons on the hexagonal lattice (Antonio Castro Neto, 2006).

2.6.1 Multi-walled Carbon Nanotubes (MWNTs)

MWNTs consist of coaxial layers, formed nanaotube cylinders of different helicities. Typical MWNT diameter is grown by arc discharge synthesis, providing ~ 3–50 nm, while CVD grown nanotubes can have much larger diameters up to 100 nm (Merkulov *et al.*, 2005). MWNTs are excellent-promising-reinforcing materials for biopolymers that have been developed for several applications such as biosensor (Guo *et al.*, 1998), and bio-electronic materials (Macdonald *et al.*, 2005).

Larger diameters of nanotubes are found in which they have a higher defect density in nanotubestructure that induce dramatically lower electrical and thermal properties. Recent studies exhibited that graphene can be used as variable and inexpensive nanofiller, substituted for CNTs (Fukushima *et al.*, 2003).

Table 2.1 Comparative chart on the mechanical, thermal and electrical properties of graphene with CNT, steel, plastic, rubber, and fiber

Materials	Tensile strength	Thermal conductivity (W/mk) at room temperature	Electrical conductivity (S/cm)
Graphene	130±10 GPa	$(4.84\pm0.44)\times10^{3}$ - $(5.30\pm0.48)\times10^{3}$	> 4000
CNT	60–100 GPa	3500	3000–4000
Nano sized steel	1769 MPa	5–6	1.35×10^{6}
Plastic (HDPE)	18–20 MPa	0.46–0.52	Insulator
Rubber (natural rubber)	20–30 MPa	0.13–0.142	Insulator
Fiber (Kevlar)	3620 MPa	0.04	Insulator

The use of multiwall carbon–nanotube (MWNT) as a reinforcement in gelatin has been studied by Li *et al.* (2003). They studied gelatin with MWNTs that can be embeded as an additive to enhance the mechanical properties of the gelatin hydrogel.

Haider *et al.* (2007) investigated the swelling of MWNT/gelatin hydrogel composites. MWNT could maintain the stability of the composites without crosslinking agent due to the hydrophobic effect of the MWNT.

Manoharan *et al.* (2009) reported that MWNT with a smaller diameter enhanced a stronger interface with the polymer matrix due to the higher surface area of the nanotube.

Ayatollahi *et al.* (2011) reported the mechanical properties of epoxy/0.5 wt% MWNT at various aspect ratios (455, 555, 715, and 1000). Both of the modulus of elasticity and the tensile strength of the samples increased with increasing of aspect ratio.

2.6.2 Graphene

Graphene, one of the elementary carbon structures (fullerene, diamond, carbon nanotube), is a single atom layer of carbon that is arranged in a two dimensional monolayer (Ionita *et al.*, 2013). It has promising properties, including high electrical conductivity at ambient temperature (Novoselov *et al.*, 2004), good thermal conductivity (Balandin *et al.*, 2008), large surface area, and outstanding mechanical properties in term of Young's modulus (Lee *et al.*, 2008). Compared with diamond, fullerene, and carbon nanotubes (CNTs), graphene is much easier to obtain and at a lower price. Thus, graphene is a suitable carbon based reinforcement filler used for enhancing mechanical performance of polymer matrix (Liang *et al.*, 2009) that have been developed for several applications such as electronic and optoelectronic devices, bio-chemical sensors, nanocomposites, and energy storage.

The use of graphene embedded in gelatin has been studied by Wang *et al.* (2012). They found that graphene/gelatin gel composites exhibit high tensile strength compared with pure gelatin films in both dry and wet states.

Liang *et al.* (2009) studied graphene/PVA nanocomposite that used graphene as a reinforcement filler. Tensile strength and young's modulus were increased by 76 % and 62 %, respectively when compared with neat PVA through the distribution of 0.7 %wt GO.

Rafiee *et al.* (2009) investigated improved mechanical properties of nanocomposites with a low graphene concentration at a weight fraction of 0.1 %. The 0.1 wt% graphene/epoxy nanocomposite possessed superior mechanical properties relative to CNT nanocomposites, namely the Young's modulus, tensile strength, and toughness since the enhanced surface area of graphene induced higher nanoparticle-matrix interaction.

2.7 Gelatin

Gelatin is a multifunctional ingredient used in many food products, including jellies, ice cream, cookies and cake. Moreover, gelatin is the primary ingredient in marsh mallows and also used as a processing aid in food industry for the clarification of cider and fruit juices. The major use of gelatin in the

pharmaceutical and the cosmetic industries is in the manufacture of capsules such as soft and two piece hard capsules (Cole, 2000; Zhang *et al.*, 2006).

There are two main types of gelatin. Type A, with isoionic point of 7 to 9, is derived from collagen with exclusively acid pretreatment. Type B, with isoionic point of 4.8 to 5.2, is the result of an alkaline pretreatment of the collagen. However, gelatin is sold with a wide range of special properties, like gel strength, to suit particular applications.Gelatin forms thermally reversible gels with water, and the gel melting temperature (<35°C) is below body temperature, which gives gelatin products unique organoleptic properties and flavour release. The disadvantage of gelatin is that it is derived from animal hide and bone (not from trotters as is a common perception), hence there are problems with regard to kosher and Halal status and vegetarians also have objections to its use. Competitive gelling agents like starch, alginate, pectin, agar, carrageenan etc. are all carbohydrates from vegetable sources, but their gels lack the melt in the mouth, elastic properties of gelatin gels.

The cross-linking of gelatin with aldehydes is being used to extend the uses of gelatin. In particular, treatment of gelatin films with glutaraldehyde (GTA) is being studied in order to improve their thermal resistance, to decrease their solubility in water, and to improve their mechanical properties. (Zhang *et al.*, 2006; Bigi *et al.*, 2001).

Bigi *et al.* (2001) studied the mechanical and thermal properties of gelatin films at different degree of glutaraldehyde crosslinking. They found an increase in stabilization of gelatin at low GTA concentration. 1 %w/w GTA is sufficient to obtain a degree of crosslinking close to 100% and as a consequence increasing of the young's modulus, thermal stability, and swelling behavior.

Yakimets *et al.* (2005) investigated mechanical properties with respect to water content of gelatin films in glassy state. The hydration of gelatin films proceeded through three main stages before reaching the glassy-rubbery transition at room temperature: (I) water bound by high energy sorption, (II) structural water, (III) polymolecular layer water. The mechanical properties of gelatin films depended on the glassy state through these three stages of hydration. For the second stage of hydration, the films improved fracture behavior, the improvement of fracture

behavior was related to the high renaturation level of gelatin films (triple helix structure).

Fukae *et al.* (2005) investigated on the gel spinning and drawing of gelatin. Gelatin fibers can be prepared by the gel spinning method using dimethyl sulfoxide as a solvent. Drawing of gelatin was effective in segmental orientation in gelatin fiber. The fibers showed high values for the mechanical properties of tensile and Young's modulus.

Li *et al.* (2006) studied the electrospinning of polyaniline-contained gelatin nanofibers for tissue engineering applications. Polyaniline, a conductive polymer, was blended with a gelatin and co-electrospun to nanofibers. Fibers were electrospun from pure gelatin and the other four sets of PAN-gelatin blend fibers with volume ratios of 15:85, 30:70, 45:55, and 60:40. The increasing amount of PAN reduced the average fiber size whereas the tensile modulus increased.

Zhang *et al.* (2006) studied the crosslinking of the electrospun gelatin nanofibers. The crosslink enhanced the thermal stability and mechanical properties, where the tensile strength and modulus were improved to nearly 10 times higher than those of electrospun membrane.

Martucci *et al.* (2006) studied the creep of glutaraldehyde-crosslinked gelatin films. Creep behavior of glutaraldehyde gelatin films was evaluated by short time flexural tests at 30 °C. Creep response decreased with increasing degree of crosslink, which indicated that crosslinking improved the film stiffness.

Gelatin is a one of viscoelastic materials derived from partial hydrolysis of native collagens, which are the most abundant structural proteins found in the animal body parts such as skin, tendon, cartilage and bone (Ward, 1977). Viscoelastic properties are often used to refer to the material chemical-microstructural relationship, as viscoelastics involve both solid-state and liquid-like behaviors (Mayer and Chawla, 2009). Studies of viscoelastic materials include stress relaxation, deformation, mechanical properties, swelling, stability, and etc (Zhang *et al.*, 2008).

2.8 Stress Relaxation

Stress relaxation is the decrease in internal stress when a material is held at a constant and finite strain. When a sufficiently small external strain is introduced to an elastic material, the applied stress causes a reversible deformation, and when the strain is removed. the residual stress rapidly relaxes to zero. Most materials are viscoelastic; when the material is subject to an external strain, a stress is generated within and the generated stress relaxes through the process of stress relaxation (Matsuoka, 1992).

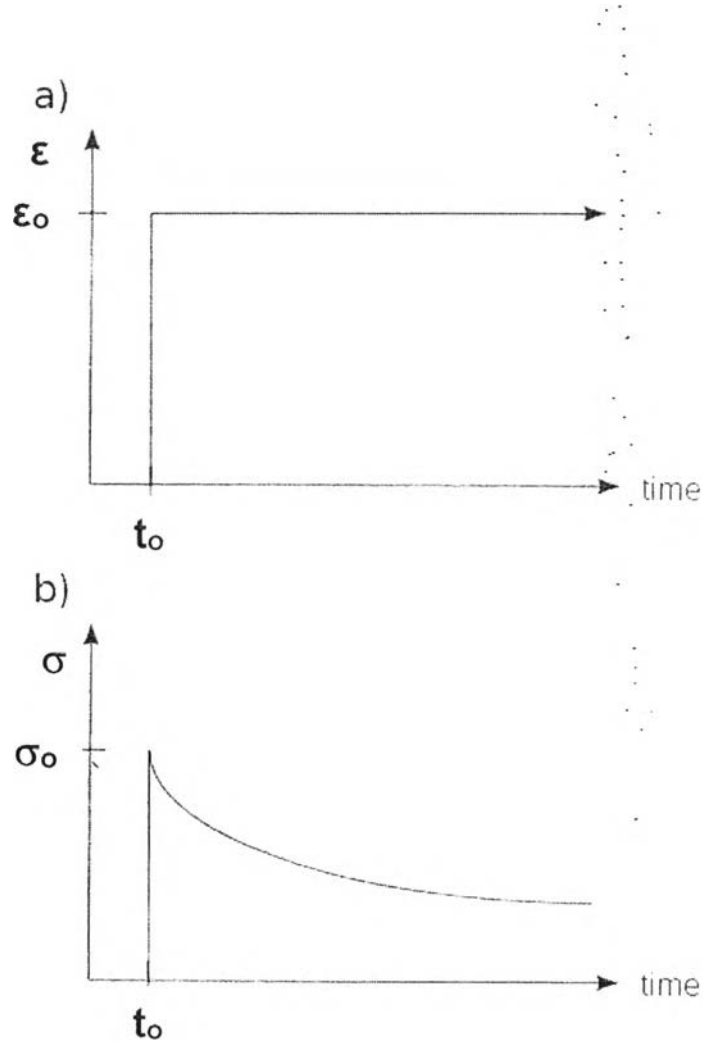

Figure 2.6 (a) Applied strain and (b) stress relaxation function for a viscoelastic material.

The simplest law for the relaxation process of viscoelastic materials is described by the Maxwell model.

$$G(t) = G_o[e^{-(t/\tau)}] \quad (2.1)$$

Equation 2.1 is a basic formula for the relaxation process, and goes beyond the Maxwell model. However, this model is not applicable towards real viscoelastic materials. In other word, the Maxwell model assumes that relaxation is a single time scale. This is not true for real polymers, since polymer molecules can perform many modes of motions, viscoelastic materials can exhibit many modes of relaxation processes. The i^{th} mode of relaxation is characterized by the relaxation time (τ_i). The relaxation modulus is the summation of all these modes of relaxation.

$$G(t) = \sum_i G_i[e^{-(t/\tau)}] \quad (2.2)$$

The relaxation processes can be divided into three stages: stage 1 is for the short time relaxation process (0-1 hr); stage 2 is for the intermediate time relaxation ($1\text{-}10^4$ hrs); and stage 3 is for the long time relaxation process ($>10^4$hrs) (Matsuoka, 1992). The Kohlrausch-Williams-Watts (KWW) equation (Williams and Watts, 1970) is a well-known equation to describe the stage1 of the stress relaxation process:

$$G(t) = G_\infty + G_o[e^{-(t/\tau)^n}] \quad (2.3)$$

where the parameter n ($0 < n \leq 1$) is often found to be approximately 0.5 for polymers, it called stretching parameter, $G(t)$ is the stress relaxation function as obtained from the experiment, G_∞ is the equilibrium modulus or the long time value, t is the experimental time, and τ is the effective relaxation time.

The KWW equation is particularly suited for described dielectric relaxation, viscoelastic relaxation in solid, hypersonic relaxation (Patterson, 1981), and dynamic bulk relaxation (Mckinney and Goldstein, 1974).

Furthermore, the effect of temperature on viscoelastic materials has been studied through the stress relaxation due to temperature dependent molecular

rearrangement processes occurring under applied stress. The relaxation process depends on the speed of the molecular motion in which temperature (T) is varied and the resultant viscoelastic functions of viscoelastic materials can be expected to depend on temperature as well as time. Thus the relaxation function may be written as $G = G(t,T)$ (Lakes, 1988).

If the relaxation times of all viscoelastic materials have the same temperature dependence, it is expected that it should be possible to superimpose linear viscoelastic data sets taken at different temperatures (Rubenstein and Colby, 2003). This is commonly known as the time–temperature superposition. Stress relaxation function data at any temperature (T) can be superimposed onto the data taken at a reference temperature (T_o) using a time scale shift factor (a_T) as in the following equation (Rubenstein and Colby, 2003):

$$a_T = \frac{\tau_i(T)}{\tau_i(T_o)} \tag{2.4}$$

where $\tau_i(T)$ and $\tau_i(T_o)$ are the characteristic time scales at T and T_o, respectively. The principle of the time-temperature superposition is based on the requirement that all time scales of the material system vary by the same factor or proportionality when temperature is varied from one to another.

Wortmann *et al.* (1995) investigated the stress relaxation and time/temperature superposition of polypropylene fiber. The result showed that the component moduli as well as the characteristic relaxation time show a pronounced temperature-dependence in which the characteristic relaxation time decreased with increasing temperature.

Palade *et al.* (1995) studied the time–temperature superposition and linear viscosity of Polybutadiene. They found that, the KWW relaxation function derived from the coupling model of Ngai and co-workers represented fairly well the loss moduli peaks from the terminal to rubbery and the softening to glassy zones. The model should be improved to obtain a better representation of both storage and loss moduli variations especially in the glassy and softening zones.

Mao *et al.* (2000) investigated the relaxation time of gelatin hydrogels at various degrees of crosslinking. The result showed the effective relaxation time shifted to a shorter amount of time as the degree of crosslinking increased. The characteristic relaxation time shifted to a shorter time as Ca^{2+} concentration increased from 4 mM to 14 mM.

Chen *et al.* (2000) investigated the time–temperature superposition of amorphous ethylene–styrene interpolymers in which the shift factor decreased as a function of temperature.

Le *et al.* (2003) studied the time dependent deformation behavior of thermoplastic elastomers. They found that temperature was an important factor determining the molecular mobility of the material. An increase in the temperature accelerated thermally activated processes and reduces relaxation times and the shift factor at different temperatures of polypropylene and nitrile rubber decreased with increasing network structure density.

Chatterjee *et al.* (2005) studied the effect of calcium cations on relaxation time distribution function of gelatin hydrogels. The result showed that the gelatin hydrogels with Ca^{2+} ions had two major peaks. The fast mode dominated the distribution spectrum with a reduction in the width of the distribution for higher concentrations of Ca^{2+} indicating growth of homogeneity in network size distribution. The mean of the fast mode relaxation time shifted to lower time scales as the calcium salt concentration was increased. However, the slow mode was less sensitive to any such change.

Meera *et al.* (2006) investigated the stress relaxation of TiO_2 and nanosilica filled rubber composites. They found that, the relaxation rate increased with increasing of TiO_2 and nanosilica loading due to the breakdown of filler-filler and weak polymer-filler networks during the course of the relaxation process. The rate of stress decay was compared for 20 phr TiO_2- and silica-filled NR. The silica-filled system showed a higher rate of stress relaxation compared to TiO_2- filled NR. This was due to the large scale filler cluster break-up in the silica-filled system.

Park *et al.* (2006) studied the time–electric field superposition in electrically activated polypropylene/layered silicate nanocomposites. They found that the electric

field reduced the time required to obtain the saturated storage modulus value of polypropylene/layered silicate nanocomposites.

Konyali *et al.* (2008) studied the long time stress relaxation of amorphous networks under uniaxial tension: The Dynamic Constrained Junction Model. The result showed that the relaxation time of polyisoprene decreased with increasing degrees of crosslinking, the relaxation was rapidly distributed throughout the crosslinking molecular segments. Increasing molecular connectivity or increasing crosslinking ratio promoted the capability of the polyisoprene to relax faster through available junctions connected with neighboring topological structures.

Zhao *et al.* (2010) studied the stress relaxation behavior in gels with ionic and covalent crosslinks. The result showed that, the stress in the gel relaxed, by different mechanisms, depending on the type of crosslinks. For a gel with ionic crosslinks, the stress relaxed as the crosslinks dissociated and reformed elsewhere, so that the network underwent plastic deformation. For a gel with covalent crosslinks, the stress relaxed as water migrated out of the gel, so that the network underwent elastic deformation.

June *et al.* (2010) studied the temperature effects in articular cartilage biomechanics. The result showed that the stress relaxation was faster at higher temperatures and the stretching parameter decreased with increasing temperature, consistent with a combination of changes in fluid viscosity and extracellular matrix polymer dynamics. Both the dynamic and equilibrium stiffness increased with temperature, consistent with polymer mechanisms.

Mitra *et al.* (2011) studied the dynamic stress relaxation behavior of nanogel filled elastomer. The result showed that the virgin elastomers, NR, and SBR showed very long-time stress relaxation process and do not reach any equilibrium within experimental time period. The time required to achieve equilibrium drastically was reduced with an increase in crosslink density in the case of crosslinked gels. In the case of crosslinked gels, the viscoelastic relaxation of an entangled dangling chain in a crosslinked polymer network occurred by a retracing mechanism in which the unattached chain end diffused towards the chain ends which were attached to the network.